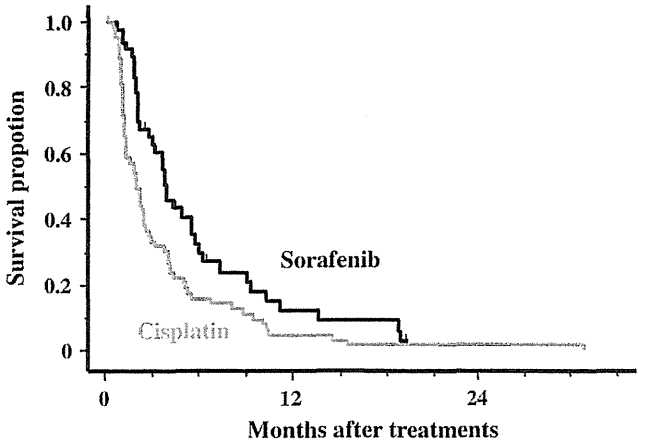

Fig. 1 Comparison of time to progression between sorafenib and hepatic arterial infusion chemotherapy using cisplatin in patients who were refractory to transcatheter arterial chemoembolization (TACE)

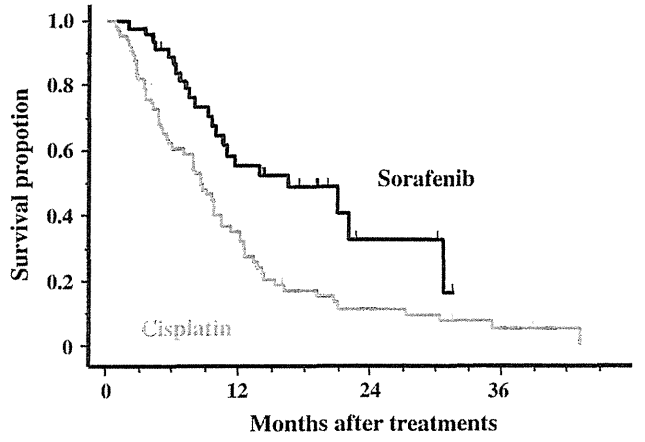

Fig. 2 Comparison of overall survival between sorafenib and hepatic arterial infusion chemotherapy using cisplatin in patients who were refractory to TACE

$P < 0.001$) (Fig. 2). The same analysis was performed for patients limited to Child–Pugh A, since sorafenib is widely recommended for the treatment of patients with Child–Pugh A. The results were similar, although the disease control rate and the time to progression were not statistically significant (data not shown).

Toxicity

Serious adverse events (SAE) occurred in two patients (1 patient, grade 4 hepatic encephalopathy; 1 patient, grade 3 erythema multiforme) in the sorafenib group, but none of the patients in the cisplatin group experienced an SAE. Thirty-eight patients (79 %) required a sorafenib dose reduction because of adverse events, such as liver dysfunction, hand-foot syndrome, or rashes, and treatment was discontinued in 7 patients (14 %) because of adverse events, such as liver dysfunction, hepatic encephalopathy, or erythema multiforme. On the other hand, none of the patients required a cisplatin dose reduction, and treatment was discontinued in 6 patients (9.1 %) because of adverse events, such as liver dysfunction, fatigue, or nausea/anorexia.

Predictive factors of time to progression and overall survival

Univariate analyses were performed to identify the factors that contributed to the prolongation of time to progression in patients who were refractory to TACE (Table 2). The univariate analyses showed that the significant factors that contributed to the prolongation of the time to progression ($P < 0.10$) were an age >65 years, a PS of 0, a maximum tumor diameter ≤3.0 cm, the absence of hepatic vein invasion, the absence of ascites, a bilirubin level ≤1.2 mg/dL, an α-fetoprotein level <1,000 ng/mL, and sorafenib treatment. A multivariate analysis was performed for the factors that showed a significant tendency ($P < 0.10$) in the univariate analysis, and the absence of hepatic vein invasion and sorafenib treatment were significant independent factors that contributed to the prolongation of the time to progression (Table 3). Univariate analyses were performed to identify the factors that contributed to survival prolongation in patients who were refractory to TACE (Table 2). The univariate analyses showed that the significant factors that contributed to the prolongation of survival ($P < 0.10$) were an age >65 years, a PS of 0, a maximum tumor diameter of ≤3.0 cm, 3 or fewer tumors, the absence of hepatic vein invasion, Child–Pugh class A, the absence of ascites, an albumin level >3.5 g/dL, a bilirubin level ≤1.2 mg/dL, an AST level <100 U/L, an α-fetoprotein level <1,000 ng/mL, a protein induced by vitamin K absence or antagonist-II (PIVKA-II) level <1,000 mAU/mL, and sorafenib treatment. A multivariate analysis was performed for the factors showing a significant tendency at $P < 0.10$, and the significant independent favorable prognosis factors were a PS of 0, 3 or fewer tumors, Child–Pugh A, an α-fetoprotein level <1,000 ng/mL, a PIVKA-II level <1,000 mAU/mL, and treatment with sorafenib (Table 3). Treatment with sorafenib had the smallest hazard ratio among these prognostic factors.

Discussion

Patients with vascular invasion, extrahepatic metastasis, and who are refractory to TACE are good candidates for sorafenib [5, 9, 10]. However, the efficacy of sorafenib in patients who are refractory to TACE has not been previously reported, although the outcome of patients with prior

Table 2 Univariate analysis of time to progression and overall survival time in patients refractory to transcatheter arterial chemoembolization treated with sorafenib or intra-arterial cisplatin

	n	Time to progression			Overall survival		
		Median (months)	Hazard ratio	*P* value	Median (months)	Hazard ratio	*P* value
Sex							
Female	19	2.9	1.01 (0.60–1.68)	0.98	10.5	0.92 (0.51–1.68)	0.79
Male	95	2.6			9.8		
Age (years)							
≤65	33	2.0	1.41 (0.92–2.14)	0.11	8.0	1.65 (1.03–2.66)	0.03
>65	81	3.0			11.4		
Performance status							
0	92	3.2	0.58 (0.35–0.95)	0.03	11.4	0.38 (0.22–0.66)	<0.001
1–2	22	1.6			4.8		
HCVAb							
Negative	37	2.8	0.82 (0.53–1.25)	0.35	9.9	0.72 (0.45–1.18)	0.19
Positive	77	2.5			9.8		
HBsAg							
Negative	99	3.0	0.86 (0.50–1.50)	0.60	9.9	1.09 (0.54–2.17)	0.82
Positive	15	2.1			9.8		
Maximum tumor diameter (cm)							
≤3.0	39	4.0	0.65 (0.43–0.99)	0.04	12.3	0.56 (0.34–0.83)	0.02
>3.0	75	2.2			8.7		
No. of tumors							
≤3	21	4.4	0.78 (0.48–1.29)	0.33	13.8	0.68 (0.39–1.19)	0.06
>3	93	2.4			8.0		
Portal vein invasion							
Present	25	3.2	0.89 (0.55–1.43)	0.62	5.4	1.34 (0.79–2.27)	0.23
Absent	89	2.6			8.7		
Hepatic vein invasion							
Present	7	2.5	2.12 (0.97–4.66)	0.05	4.8	2.17 (0.94–5.03)	0.13
Absent	107	2.8			9.2		
Stage[a]							
II or III	87	2.8	0.94 (0.59–1.48)	0.77	11.6	0.64 (0.39–1.07)	0.08
IV	27	2.5			6.2		
Child–Pugh class							
A	68	3.2	0.84 (0.56–1.26)	0.39	9.5	0.65 (0.41–1.01)	0.08
B	46	2.2			7.8		
Ascites							
Present	26	2.2	1.56 (0.98–2.47)	0.06	5.6	2.15 (1.32–3.53)	0.01
Absent	88	2.9			9.2		
Albumin (g/dL)							
≤3.5	76	2.4	1.17 (0.78–1.77)	0.44	7.8	1.90 (1.16–3.11)	0.02
>3.5	38	3.8			10.6		
Total bilirubin (mg/dL)							
≤1.2	81	3.2	0.66 (0.42–1.02)	0.06	11.6	0.42 (0.26–0.66)	<0.001
>1.2	33	1.6			4.8		
Prothrombin time (%)							
<70	42	2.9	0.95 (0.63–1.42)	0.79	10.5	0.93 (0.59–1.47)	0.77
≥70	72	2.5			9.9		

Table 2 continued

	n	Time to progression			Overall survival		
		Median (months)	Hazard ratio	*P* value	Median (months)	Hazard ratio	*P* value
AST (U/L)							
<100	82	3.0	0.86 (0.55–1.35)	0.50	12.3	0.44 (0.27–0.70)	<0.001
≥100	32	2.2			5.5		
ALT (U/L)							
<100	97	2.6	0.90 (0.52–1.56)	0.70	9.9	0.85 (0.44–1.57)	0.59
≥100	17	2.5			8.5		
α-Fetoprotein (ng/mL)							
<1,000	71	3.8	0.60 (0.40–0.91)	0.01	12.2	0.61 (0.39–0.96)	0.03
≥1,000	43	2.1			7.1		
PIVKA-II (mAU/mL)							
<1,000	67	3.1	0.78 (0.52–1.16)	0.22	10.6	0.62 (0.40–0.96)	0.03
≥1,000	45	2.1			9.5		
Treatments							
Sorafenib	48	3.9	0.57 (0.38–0.86)	0.01	16.4	0.44 (0.27–0.72)	<0.001
Cisplatin	66	2.0			8.6		

HCVAb hepatitis C viral antibody, *HBsAg* hepatitis B surface antigen, *AST* aspartate aminotransferase, *ALT* alanine aminotransferase, *PIVKAII* protein induced by vitamin K absence or antagonists-II

[a] Japanese classification of primary liver cancer

Table 3 Multivariate analysis of overall survival and time to progression in patients refractory to TACE

	Hazard ratio	*P* value
Time to progression		
Hepatic vein invasion: present	0.41 (0.19–0.91)	0.03
Treatment: sorafenib	0.55 (0.37–0.83)	0.004
Overall survival		
Performance status: 0	0.46 (0.27–0.81)	0.006
No. of tumors: ≤3	0.51 (0.29–0.91)	0.02
Child–Pugh class: A	0.44 (0.27–0.71)	0.001
α-Fetoprotein: <1,000 ng/mL	0.52 (0.22–0.84)	0.008
PIVKA-II: <1,000 mAU/mL	0.47 (0.29–0.76)	0.002
Treatment: sorafenib	0.42 (0.25–0.77)	0.001

TACE has been reported [11, 12]. We retrospectively evaluated the efficacy of sorafenib in patients who were refractory to TACE. The following data were obtained: the response rate (CR + PR) was 6.3 %, the disease control rate (CD + PR + SD) was 60.4 %, and the median time to progression was 3.9 months; these results were comparable to those obtained for sorafenib to date [7, 8]. The median survival time of 16.4 months was regarded as favorable. The patients who were refractory to TACE have a lower frequency of vascular invasion, which is a significant predictor of a poor prognosis in patients with advanced HCC. In addition, most of the TACE refractory patients had an intermediate BCLC stage. The TACE refractory patients in this study (proportion of advanced stage 33 %) had a better BCLC stage than the patients in previous trials (proportion of advanced stage SHARP, 82 %; Asia-Pacific trial, 95.3 %). Favorable tendencies, therefore, might be shown for the overall survival of a subgroup of patients who are refractory to TACE among advanced HCC patients in whom sorafenib treatment is indicated.

A definition of "refractory to TACE" has not yet been established. In this study, the definition of "refractory to TACE" was regarded as progression or a tumor shrinkage rate of <25 % in hypervascular lesions as visualized using dynamic CT and/or MRI after 1–3 months of TACE. According to the consensus-based clinical practice guidelines proposed by the Japan Society of Hepatology 2010 [5], however, "refractory to TACE" is defined as two or over consecutive incomplete necrotic reactions or the appearance of a new lesion, vascular invasion, or extrahepatic metastases. Although a consensus has not been reached among clinicians, this is a critical issue when considering a conversion from TACE to sorafenib treatment in patients with unresectable HCC.

In the present study, sorafenib was compared with hepatic arterial infusion chemotherapy using cisplatin, which was used before the introduction of sorafenib. A consensus on a standard therapy has not been attained for hepatic arterial infusion chemotherapy, since its survival benefit has not been elucidated [10]. However, this regimen is still frequently used in Japan, because favorable antitumor effects and long-term survivals have been seen in a

few patients [15–21]. Nonetheless, hepatic arterial infusion chemotherapy has not been reported to have favorable results in patients who are refractory to TACE [13, 14]. Regarding hepatic arterial infusion chemotherapy using cisplatin in patients who were refractory to TACE ($n = 84$), the response rate at out-patient hospitals was 3.6 %, the median time to progression was 1.7 months, and the median overall survival period was 7.1 months [13], while the results of a phase II study of hepatic arterial infusion chemotherapy using cisplatin in patients with unresectable HCC ($n = 80$) were favorable, with a response rate of 33.8 % and a 1-year survival rate of 67.5 % [15]. One possible reason for the difference between these studies might be differences in the characteristics of the study populations. Most patients in the phase II trial of cisplatin were TACE-naïve, whereas only patients with TACE-refractory disease were included in the present study. Thus, hepatic arterial infusion chemotherapy may not be expected to show favorable therapeutic results when the patients are limited to those refractory to TACE, although the reason remains unknown. Therefore, the results were compared with those for patients who were refractory to TACE and were treated with sorafenib. Although the patient age was significantly higher in the sorafenib group and the PS and tumor size was slightly worse in the cisplatin group, no other significant differences in the patient characteristics were observed between the two groups. The response rate was comparable, but the sorafenib group showed significantly higher results for the disease control rate, time to progression, and overall survival. We also performed a multivariate analysis to examine the factors that contributed to the time to progression and overall survival in patients who were refractory to TACE, and treatment with sorafenib was one of the significant factors. These results suggest that sorafenib, rather than hepatic arterial infusion chemotherapy using cisplatin, might be the treatment of first choice in patients who are refractory to TACE. This outcome might not have much impact in overseas settings, where hepatic arterial infusion chemotherapy is less popular, but it is quite disappointing in Japan, since hepatic arterial infusion chemotherapy using cisplatin was expected to show a therapeutic effect comparable to that of sorafenib.

The present study has some limitations. First, the results for sorafenib treatment in patients who were refractory to TACE were obtained as part of a single-site, retrospective study. A prospective study enrolling only patients who are refractory to TACE should be performed in the future to verify the efficacy of sorafenib in patients who are refractory to TACE. Second, the periods of treatment differed between the sorafenib group and the cisplatin group. Third, the influence of subsequent treatment on the overall survival cannot be denied. Hepatic arterial infusion chemotherapy using cisplatin was administered as a subsequent treatment in 7 patients in the sorafenib group, whereas patients in the cisplatin group were not treated with sorafenib. Still, the anti-tumor effect of hepatic arterial infusion chemotherapy using cisplatin following sorafenib was PD in all the patients, and the impact would have been negligible. Finally, considering the possible selection bias in therapeutic policy after the introduction of sorafenib, we selected patients with different periods of treatment, but the results might also have been affected by the difference in periods. Also, no significant differences in the patient characteristics, except for age, total bilirubin, and AST, were seen between the sorafenib and the hepatic arterial infusion chemotherapy using cisplatin group, but subtle differences in the patient characteristics might have affected the favorable results for sorafenib, since this study was a retrospective comparison.

In conclusion, sorafenib showed a favorable efficacy in patients who were refractory to TACE, resulting in a significantly higher disease control rate, longer time to progression, and longer overall survival compared with hepatic arterial infusion chemotherapy using cisplatin. Thus, sorafenib, rather than hepatic arterial infusion chemotherapy, should be considered as the first-line therapy for patients who are refractory to TACE in the future.

Acknowledgments This work was supported in part by Grants-in-Aid for Cancer Research and for the Third-Term Comprehensive 10-Year Strategy for Cancer Control from the Ministry of Health, Labour, and Welfare of Japan.

Conflict of interest The authors declare that they have no conflict of interest.

References

1. Kudo M, Izumi N, Kokudo N, Matsui O, Sakamoto M, Nakashima O, et al. Management of hepatocellular carcinoma in Japan: consensus-based clinical practice guidelines proposed by the Japan Society of Hepatology (JSH) 2010 updated version. Dig Dis. 2011;29:339–64.
2. Bruix J, Sherman M, Practice Guidelines Committee, American Association for the Study of Liver Diseases. Management of hepatocellular carcinoma. Hepatology. 2005;42:1208–36.
3. Cammà C, Schepis F, Orlando A, Albanese M, Shahied L, Trevisani F, et al. Transarterial chemoembolization for unresectable hepatocellular carcinoma: meta-analysis of randomized controlled trials. Radiology. 2002;224:47–54.
4. Llovet JM, Bruix J. Systematic review of randomized trials for unresectable hepatocellular carcinoma: chemoembolization improves survival. Hepatology. 2003;37:429–42.
5. Llovet JM, Bruix J. Molecular targeted therapies in hepatocellular carcinoma. Hepatology. 2008;48:1312–27.
6. Zhu AX. Development of sorafenib and other molecularly targeted agents in hepatocellular carcinoma. Cancer. 2008;112:250–9.
7. Llovet JM, Ricci S, Mazzaferro V, Hilgard P, Gane E, Blanc JF, et al. Sorafenib in advanced hepatocellular carcinoma. N Engl J Med. 2008;359:378–90.

8. Cheng AL, Kang YK, Chen Z, Tsao CJ, Qin S, Kim JS, et al. Efficacy and safety of sorafenib in patients in the Asia-Pacific region with advanced hepatocellular carcinoma: a phase III randomised, double-blind, placebo-controlled trial. Lancet Oncol. 2009;10:25–34.
9. Kudo M, Izumi N, Kokudo N, Matsui O, Sakamoto M, Nakashima O, et al. Management of hepatocellular carcinoma in Japan: consensus-based clinical practice guidelines proposed by the Japan Society of Hepatology (JSH) 2010 updated version. Dig Dis. 2011;29:339–64.
10. Yamashita T, Kaneko S. Treatment strategies for hepatocellular carcinoma in Japan. Hepatol Res. 2013;43:44–50.
11. Bruix J, Raoul JL, Sherman M, Mazzaferro V, Bolondi L, Craxi A, et al. Efficacy and safety of sorafenib in patients with advanced hepatocellular carcinoma: subanalyses of a phase III trial. J Hepatol. 2012;57:821–90.
12. Cheng AL, Guan Z, Chen Z, Tsao CJ, Qin S, Kim JS, et al. Efficacy and safety of sorafenib in patients with advanced hepatocellular carcinoma according to baseline status: subset analyses of the phase III Sorafenib Asia-Pacific trial. Eur J Cancer. 2012;48:1452–65.
13. Iwasa S, Ikeda M, Okusaka T, Ueno H, Morizane C, Nakachi K, et al. Transcatheter arterial infusion chemotherapy with a fine-powder formulation of cisplatin for advanced hepatocellular carcinoma refractory to transcatheter arterial chemoembolization. Jpn J Clin Oncol. 2011;41:770–5.
14. Kirikoshi H, Yoneda M, Mawatari H, Fujita K, Imajo K, Kato S, et al. Is hepatic arterial infusion chemotherapy effective treatment for advanced hepatocellular carcinoma resistant to transarterial chemoembolization? World J Gastroenterol. 2012;18:1933–9.
15. Yoshikawa M, Ono N, Yodono H, Ichida T, Nakamura H. Phase II study of hepatic arterial infusion of a fine-powder formulation of cisplatin for advanced hepatocellular carcinoma. Hepatol Res. 2008;38:474–83.
16. Court WS, Order SE, Siegel JA, Johnson E, DeNittis AS, Principato R, et al. Remission and survival following monthly intraarterial cisplatinum in nonresectable hepatoma. Cancer Invest. 2002;20:613–25.
17. Ueshima K, Kudo M, Takita M, Nagai T, Tatsumi C, Ueda T, et al. Hepatic arterial infusion chemotherapy using low-dose 5-fluorouracil and cisplatin for advanced hepatocellular carcinoma. Oncology. 2010;78(Suppl 1):148–53.
18. Yamasaki T, Kimura T, Kurokawa F, Aoyama K, Ishikawa T, Tajima K, et al. Prognostic factors in patients with advanced hepatocellular carcinoma receiving hepatic arterial infusion chemotherapy. J Gastroenterol. 2005;40:70–8.
19. Obi S, Yoshida H, Toune R, Unuma T, Kanda M, Sato S, et al. Combination therapy of intraarterial 5-fluorouracil and systemic interferon-alpha for advanced hepatocellular carcinoma with portal venous invasion. Cancer. 2006;106:1990–7.
20. Uka K, Aikata H, Takaki S, Miki D, Kawaoka T, Jeong SC, et al. Pretreatment predictor of response, time to progression, and survival to intraarterial 5-fluorouracil/interferon combination therapy in patients with advanced hepatocellular carcinoma. J Gastroenterol. 2007;42:845–53.
21. Monden M, Sakon M, Sakata Y, Ueda Y, Hashimura E, FAIT Research Group. 5-Fluorouracil arterial infusion + interferon therapy for highly advanced hepatocellular carcinoma: a multicenter, randomized, phase II study. Hepatol Res. 2012;42:150–65.
22. Therasse P, Arbuck SG, Eisenhauer EA, Wanders J, Kaplan RS, Rubinstein L, et al. New guidelines to evaluate the response to treatment in solid tumors. European Organization for Research and Treatment of Cancer, National Cancer Institute of the United States, National Cancer Institute of Canada. J Natl Cancer Inst. 2000;92:205–16.

European Journal of Radiology 83 (2014) e23–e35

Contents lists available at ScienceDirect

European Journal of Radiology

journal homepage: www.elsevier.com/locate/ejrad

Review

Primary staging of laryngeal and hypopharyngeal cancer: CT, MR imaging and dual-energy CT

Hirofumi Kuno[a,*], Hiroaki Onaya[b,1], Satoshi Fujii[c,2], Hiroya Ojiri[d,3], Katharina Otani[e,4], Mitsuo Satake[a,5]

[a] Diagnostic Radiology Division, National Cancer Center Hospital East, 6-5-1, Kashiwanoha, Kashiwa, Chiba 277-8577, Japan
[b] Diagnostic Radiology Division, National Cancer Center Hospital, 5-1-1 Tsukiji Chuo-ku, Tokyo 104-0045, Japan
[c] Pathology Division, Research Center for Innovative Oncology, National Cancer Center Hospital East, 6-5-1 Kashiwanoha, Kashiwa, Chiba 277-8577, Japan
[d] Department of Radiology, Jikei University School of Medicine, 3-25-18 Nishi-shinbashi Minato-ku, Tokyo 105-8461, Japan
[e] Imaging & Therapy Systems Division, Siemens Japan K.K., Gate City Osaki West Tower 1-11-1 Osaki, Shinagawa-ku, Tokyo 141-8644, Japan

ARTICLE INFO

Article history:
Received 12 April 2013
Received in revised form 23 July 2013
Accepted 20 October 2013

Keywords:
Laryngeal cancer
Hypopharyngeal cancer
Computed tomography
Magnetic resonance imaging
Dual-energy CT
Staging

ABSTRACT

Laryngeal and hypopharyngeal cancer, in particular T4a disease associated with cartilage invasion and extralaryngeal spread, needs to be evaluated accurately because treatment can impact heavily on a patient's quality of life. Reliable imaging tools are therefore indispensible. CT offers high spatial and temporal resolution and remains the preferred imaging modality. Although cartilage invasion can be diagnosed with acceptable accuracy by applying defined criteria for combinations of erosion, lysis and transmural extralaryngeal spread, iodine-enhanced tumors and non-ossified cartilage are sometimes difficult to distinguish. MR offers high contrast resolution for images without motion artifacts, although inflammatory changes in cartilage sometimes resemble cartilage invasion. With dual-energy CT, combined iodine overlay images and weighted average images can be used for evaluation of cartilage invasion, since iodine enhancement is evident in tumor tissue but not in cartilage. Extralaryngeal spread can be evaluated from CT, MR or dual-energy CT images and the routes of tumor spread into the extralaryngeal soft tissue must be considered; (1) via the thyrohyoid membrane along the superior laryngeal neurovascular bundle, (2) via the inferior pharyngeal constrictor muscle, and (3) via the cricothyroid membrane. Radiologists need to understand the advantages and limitations of each imaging modality for staging of laryngeal and hypopharyngeal cancer.

1. Introduction

Laryngeal and hypopharyngeal cancers are common malignant tumors in the head and neck, and most of such cases are squamous cell carcinomas [1]. In view of the functional and social importance of the larynx, any decision about the optimal management strategy for laryngeal or hypopharyngeal cancer must involve consideration of both potential survival and the functional consequences of any given treatment approach. Patients with T1, T2 and limited cartilage invasion disease can be considered positively for organ-preserving procedures such as radiation therapy alone, a combination of chemotherapy and radiation therapy, and function-preserving partial laryngectomy procedures [2–6]. Patients with T4a disease, particularly when the tumor extends through the cartilage into the soft tissue of the neck, often need aggressive treatments such as total laryngectomy [2,7,8], because the risks of recurrence and cartilage necrosis after radiotherapy alone are high [2–4]. Both CT and MR imaging are routinely used to differentiate between limited and gross cartilage invasion. However, cartilage invasion is sometimes overestimated, resulting in unnecessary total laryngectomies in some patients [9,10].

Currently, dual-energy CT is being investigated in several clinical fields [11–15], including the evaluation of head and neck cancer [16]. Since treatment is decided according to the precise extent and invasion pattern of a tumor, the findings of these imaging procedures play a crucial role in any multidisciplinary approach for management of laryngeal and hypopharyngeal cancer [17–19]. Rapid technological developments in recent years have made it necessary for all members of multidisciplinary teams to understand the

* Corresponding author. Tel.: +81 4 7133 1111x91311; fax: +81 4 7131 4724.
E-mail addresses: hkuno@east.ncc.go.jp (H. Kuno), honaya@ncc.go.jp (H. Onaya), sfujii@east.ncc.go.jp (S. Fujii), ojiri@jikei.ac.jp (H. Ojiri), katharina.otani@siemens.com (K. Otani), msatake@east.ncc.go.jp (M. Satake).
[1] Tel.: +81 3 3542 2511.
[2] Tel.: +81 4 7133 1111.
[3] Tel.: +81 3 3433 1111.
[4] Tel.: +81 3 3493 7429.
[5] Tel.: +81 4 7133 1111.

0720-048X/$ – see front matter © 2013 Elsevier Ireland Ltd. All rights reserved.
http://dx.doi.org/10.1016/j.ejrad.2013.10.022

Table 1
Primary tumor (T) staging according to the American Joint Committee on Cancer (AJCC) 7th edition (modified version by author).

	Laryngeal cancer			Hypopharyngeal cancer
	Supraglottic	Glottic	Subglottic	
T1	One subsite	(a) One vocal cord (b) both vocal cords	Limited to subglottis	≤2 cm and limited to one subsite
T2	More than one subsite	Extends to supra/sub glottis Impaired vocal cord mobility	Extends to glottis	>2–4 cm or more than one subsite
T3	PGS/PES or vocal cord fixation Inner cortex of thyroid cartilage Extends to postcricoid	PGS or vocal cord fixation Inner cortex of thyroid cartilage	Vocal cord fixation	>4 cm or vocal cord fixation
T4a	Tumor invades through the thyroid cartilage or extra-laryngeal spread		Tumor invades thyroid/cricoid cartilage or extra-laryngeal spread	
T4b	Tumor invades prevertebral space, encases carotid artery, or invades mediastinal structures			

Note: PGS = paraglottic space; PES = preepiglottic space.

potential applications, limitations, and appropriate criteria of these imaging modalities.

In this article, we review the significant role of imaging for staging of laryngeal and hypopharyngeal cancer. We discuss the appearances of T4a disease on conventional CT and MR images and illustrate how dual-energy CT can be applied for evaluation of laryngeal and hypopharyngeal cancer.

2. Primary tumor staging (T) of laryngeal and hypopharyngeal cancer

The system for staging of primary laryngeal (glottic, supraglottic and subglottic) and hypopharyngeal cancer is outlined in Table 1 (American Joint Committee on Cancer 2010) [20]. Clinical staging of the primary site is based on involvement of various subsites of the larynx or adjacent regions of the pharynx and vocal cord mobility. Assessment of the primary tumor is initially accomplished by clinical inspection, using indirect mirror and direct endoscopic examination with a fiberoptic nasolaryngoscope. However, these tumors have a tendency to spread submucosally, and this extension into deeply seated tissue planes can be easily missed by clinical examination alone [8,17,19]. Therefore, clinicians rely on imaging to predict which patients will have T3–4 disease. Even if the primary tumor has been clinically diagnosed as T1–2 disease on the basis of inspection, imaging is an important adjunct to exclude any T3–4 factor features or the presence of submucosal extension [8,21–23]. Therefore, cross-sectional imaging using CT or MR imaging is mandatory for completing the staging process, and should be included in the diagnostic workup.

For laryngeal cancer, the first imaging criterion that defines T3 lesions is extension into the paraglottic and/or preepiglottic space, irrespective of vocal cord mobility. In addition, tumor erosion limited to the inner cortex of the thyroid cartilage indicates a T3 lesion, whereas erosion of the outer cortex of the thyroid cartilage define a T4a tumor. For hypopharyngeal cancer, unlike the larynx, criteria that define T3 lesions are based on vocal cord mobility and tumor diameter only. Hypopharyngeal cancer with invasion of the thyroid or cricoid cartilage indicates a T4a lesion, even in cases of localized cartilage invasion. In any event, accurate staging requires diagnosis of subtle cartilage invasion.

Extralaryngeal tumor spread is also one of the important predictors of T4a disease, with or without cartilage invasion, in laryngeal and hypopharyngeal cancer.

3. Technical considerations for CT, MR imaging and dual-energy CT

3.1. Conventional CT

CT is the preferred imaging method for staging of laryngeal and hypopharyngeal cancer. The images are obtained with the patient supine and during quiet respiration (not while holding the breath). The neck should be in slight extension, and the head is aligned along the cephalocaudal axis to allow comparison of symmetrical structures. Malpositioning may create an appearance that simulates disease. Every effort should be made to make the patient feel comfortable. When a small tumor is suspected, the patient may be scanned during a modified Vasalva maneuver or during phonation to open the piriform sinuses [24,25]. Typically, a 100-mL injection of 300 mgI/mL iodinated contrast medium is injected at a rate of 2.5 mL/s and the scan is initiated 70 s after the start of the injection, proceeding in a cranio-caudal direction. The scan range is set from the base of the skull to the bottom of the neck. Reconstructed images are generated as frontal and coronal sections parallel and vertical to the vocal cords from 1 cm above the hyoid bone to the inferior margin of the cricoid cartilage (2-mm thickness and 16-cm field of view).

3.2. MR imaging

MR imaging is also obtained with the patient supine and during quiet respiration. Axial T2-weighted fast spin echo (FSE) and T1-weighted FSE images are obtained with a scan orientation parallel to the true vocal cords. Typical image parameters for a standard examination include a slice thickness of 3 mm with a 1-mm intersection gap. Additional axial fat-saturated T1-weighted fast field echo (FFE) images after intravenous administration of gadolinium chelates are obtained routinely. When evaluations using CT alone are insufficient to determine cartilage invasion, the following 3D sequences are additionally performed within the area from 1 cm above the hyoid bone to the inferior margin of the cricoid cartilage: a 3D-T2-weighted image (3D-T2WI) is acquired in the transverse plane with a 3D volume isotropic T2-weighted acquisition (VISTA) sequence (TR/TE, 1,100/91 with Driven Equilibrium [DRIVE] technique; flip angle, 90; field of view, 230 mm; matrix, 190 × 448; slice thickness/gap, 1.5 mm/0 mm). A 3D-T1-weighted image (3D-T1WI) is then acquired in the transverse plane with a 3D Turbo Field Echo (TFE) sequence unenhanced (TR/TE, 6/2.3; flip angle,

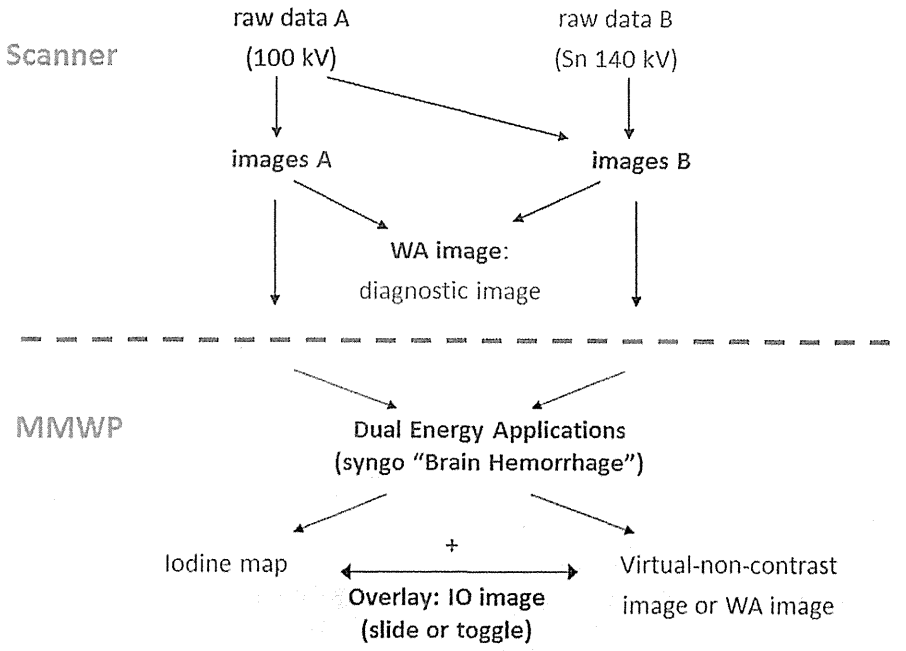

Fig. 1. Flow chart showing an overview of post-processing. Weighted-average (WA) CT images are generated by fusing data sets acquired with different tube voltages (100 and 140 kV). WA images resemble conventional CT images. Iodine overlay (IO) images are generated by fusing virtual non-contrast images and iodine images at a ratio of 0.5.

15; field of view, 230 mm; matrix, 224 × 224; slice thickness/gap, 1.0 mm/0 mm) and fat saturated contrast-enhanced (TR/TE, 6/1.15; flip angle, 15; field of view, 230 mm; matrix, 224 × 224; slice thickness/gap, 1.0 mm/0 mm). Images in the coronal or sagittal plane may be obtained in order to evaluate certain anatomic spaces, such as the preepiglottic space in the sagittal plane, or the paraglottic space and the ventricle in the coronal plane.

3.3. Dual-energy CT

3.3.1. Basic principles

Single-energy CT generates images based on the X-ray absorption coefficient of scanned tissues, and according to their density the tissues are assigned a CT value and displayed as a grey scale. As a result, it may be difficult to differentiate materials of different chemical composition, such as iodine and bone or iodine-enhanced lesions and cartilage, as they have the same CT value on CT images [8,26]. This difficulty can be overcome for some materials using dual-energy CT [15,27,28] which exploits the dependence of the absorption coefficient on the energy of the X-ray spectrum, or kV setting, used for the scan [13,29–31]. For example, materials such as iodine have lower CT values at high X-ray energies than at low X-ray energies, whereas fat tissue shows the opposite behavior. The CT value of water, soft tissue and blood stays almost constant at all X-ray energies.

In practice, two CT images taken at different tube voltages, typically 80 or 100 kV and 140 kV, are sufficient to classify many tissues. Different scan techniques have been developed to acquire dual-energy CT data sets; dual-source dual-energy CT, dual-energy CT with fast kilovolt switching, and multilayered-detector dual-energy CT [32,33]. Here, we limit our discussion to dual-source dual-energy CT [33,34], used at our institution.

Several algorithms can be used to extract material information and generate material maps or remove materials from images. A three-material decomposition algorithm applied to each voxel of an iodine-enhanced dual-energy CT image set makes it possible to compute iodine maps and virtual non-contrast images. Three materials have to be predefined for this algorithm according to the scanned body area: for example iodine, soft tissue and air are chosen for lung imaging [14], and iodine, fat and tissue for liver imaging [33]. For the head-neck region, the materials are set to iodine, brain parenchyma and hemorrhage [12,16].

3.3.2. Dual-energy CT protocol

For dual-source dual-energy CT scans using 128-slice dual-source CT (SOMATOM Definition Flash; Siemens Healthcare, Forchheim, Germany), the following parameters are applied: 100 and 140 kV tube voltages with a 0.4-mm tin filter (labeled as Sn140 kV), 200 and 200 effective mAs, 0.33-s rotation time, 32 × 0.6-mm collimation with a z-flying focal spot, and a pitch of 0.6. The tin filter blocks low-energy X-rays from the 140 kV spectrum, thus reducing radiation to the patient and enhancing energy separation of X-rays from the low and high kV X-ray tubes. These parameters result in an average CT dose index of 14–15 mGy, which is equivalent to that of single-energy CT scans. Noise needs to be minimized to ensure precise three-material decomposition in the head and neck, where many heterogeneous structures such as cartilage, soft tissues and air in the trachea require a high image resolution. A voltage combination of 100 kV and Sn140 kV, rather than 80 and 140 kV, is chosen to minimize noise while maximizing the separation of the X-ray tubes' energy spectra. The methods of contrast material injection are the same as for conventional CT.

3.3.3. Image reconstruction and post-processing

The image reconstruction and post-processing flow is shown in Fig. 1: two sets of raw data (100 kV and Sn140 kV) are separately reconstructed from the acquired dual-energy data using a 1-mm slice thickness and 0.7-mm increment, and a third, WA image set is generated at the same time, linearly weighing and fusing each pixel of the 100-kV and Sn140 kV data (p100 and p140, respectively) at the default ratio of $w = 0.5$ according to the following formula: $[w \times \text{p100}] + [(1 - w) \times \text{p140}]$. A medium sharp D30f kernel is applied for all reconstructions. WA images are used as diagnostic images since they are equivalent in terms of image quality to single-energy 120 kV CT images [35,36].

Next, the images are post-processed on a separate workstation (MMWP; Siemens Healthcare), and three-material-decomposition analysis (Syngo Dual Energy, Brain Hemorrhage; Siemens

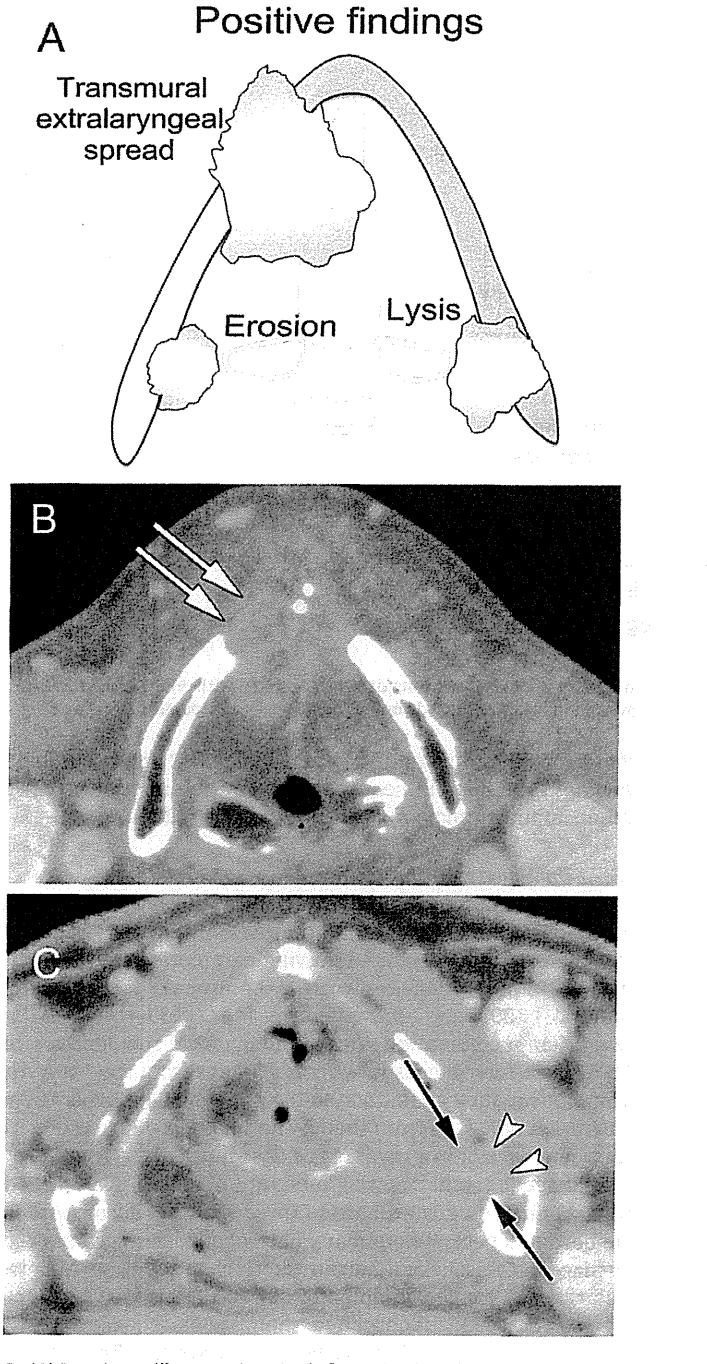

Fig. 2. (A) Drawing to illustrate the criteria for evaluation of thyroid cartilage invasion. Erosion is defined as invasion beyond the inner cortex without reaching the outer cortex (less than half of the cartilage width), lysis is defined as almost reaching the outer cortex but with preservation of the cortex, and extralaryngeal spread is defined as all-layer invasion through both the inner and outer cortex (penetration) of the cartilage, including the extralaryngeal soft tissues. (B) Positive finding of invasion through the outer cortex of the thyroid cartilage in a 56-year-old man with glottic cancer. Axial contrast-enhanced CT image at the level of the vocal cords shows tumor invasion into the thyroid cartilage, spreading into the extralaryngeal soft tissue (white arrows). (C) Positive finding of thyroid cartilage lysis in a 69-year-old man with hypopharyngeal cancer. Axial contrast-enhanced CT image at the glottic level shows a tumor mass arising from the left piriform sinus. The inner cortex of the left thyroid cartilage shows disappearance of a thin hypo-attenuated line between the tumor and the cartilage (arrows), and substitution of cartilage with tumor tissue as demonstrated by CT attenuation (arrowheads).

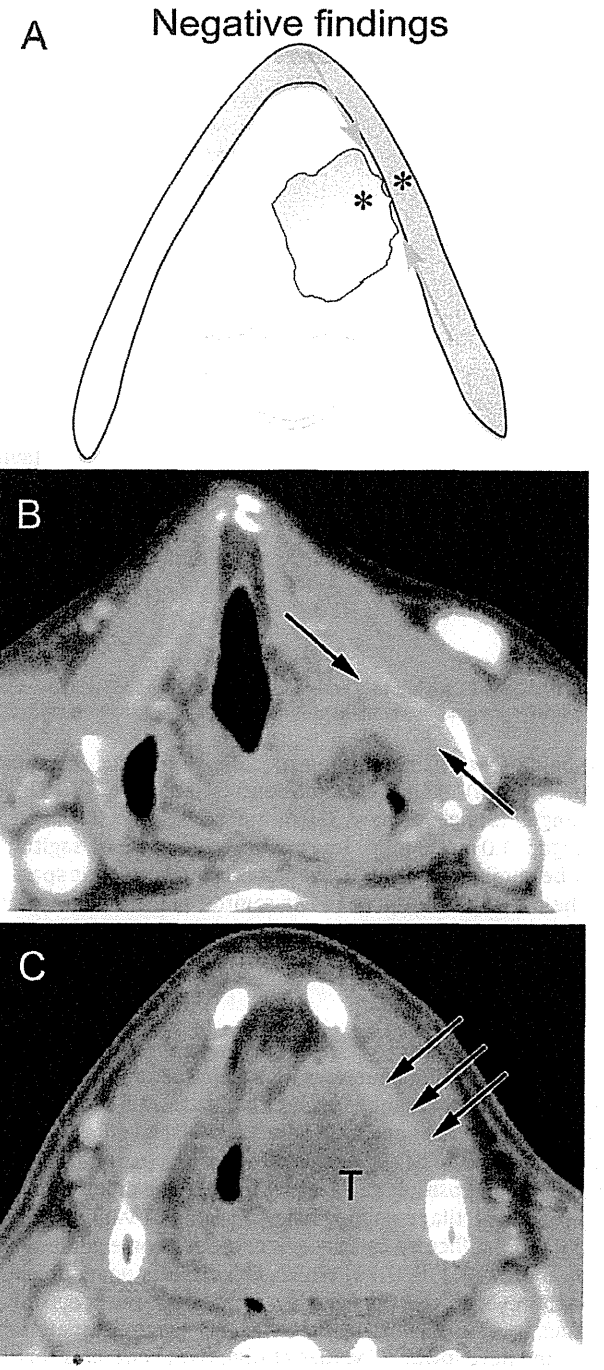

Fig. 3. (A) Drawing to illustrate the criteria for negative thyroid cartilage invasion based on two concurrent findings: (1) perfect or almost continuously defined thin hypo-attenuated line between the tumor and the cartilage (arrows), (2) difference in CT attenuation between non-ossifying cartilage and the tumor (asterisks). (B) Negative finding of thyroid cartilage invasion in a 67-year-old man with hypopharyngeal cancer. Axial contrast-enhanced CT image at the level of the false vocal cords shows a tumor mass arising from the left piriform sinus, but preservation of a dark line between the tumor and the cartilage is evident (arrows). (C) Negative finding of thyroid cartilage invasion in a 61-year-old man with hypopharyngeal cancer. Axial contrast-enhanced CT image at the supraglottic level shows a tumor mass arising from the left piriform sinus. CT attenuation of the non-ossifying cartilage (arrows) is different from that of the tumor (T).

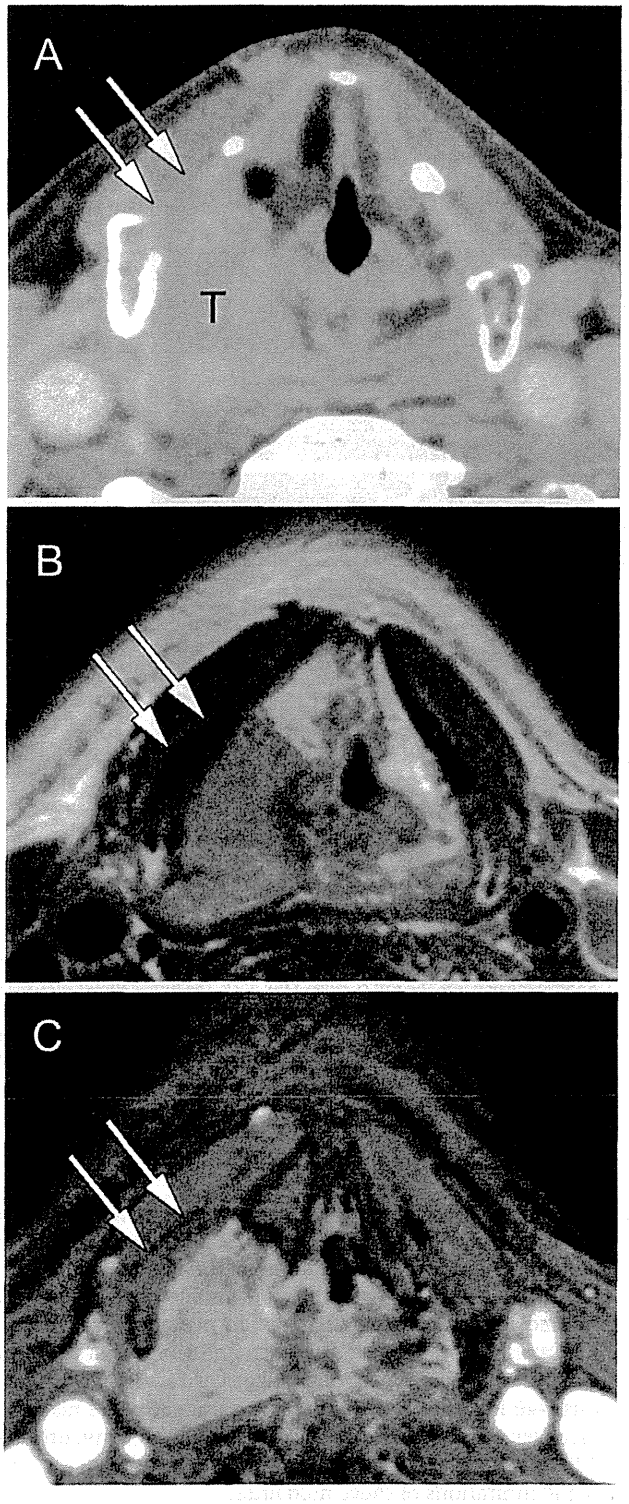

Fig. 4. True negative finding for thyroid cartilage invasion by MR imaging in a 69-year-old man with hypopharyngeal cancer. (A) Axial contrast-enhanced CT image at the level of the false vocal cords shows tumor mass (T) arising from the right piriform sinus. The tumor is located adjacent to non-ossified cartilage of the right thyroid lamina, and the tumor and cartilage show similar CT values, making them almost indistinguishable (arrows). (B) T2-weighted MR image obtained at the same level shows a right-sided piriform sinus tumor with intermediate signal intensity. The adjacent right thyroid lamina can be differentiated by its low signal intensity (arrows). (C) Fat-suppressed contrast-enhanced T1-weighted image shows contrast enhancement of the tumor mass and poor enhancement of the thyroid lamina (arrows) relative to the adjacent tumor mass. Pathological findings confirmed that there was no tumor cell infiltration into the cartilage.

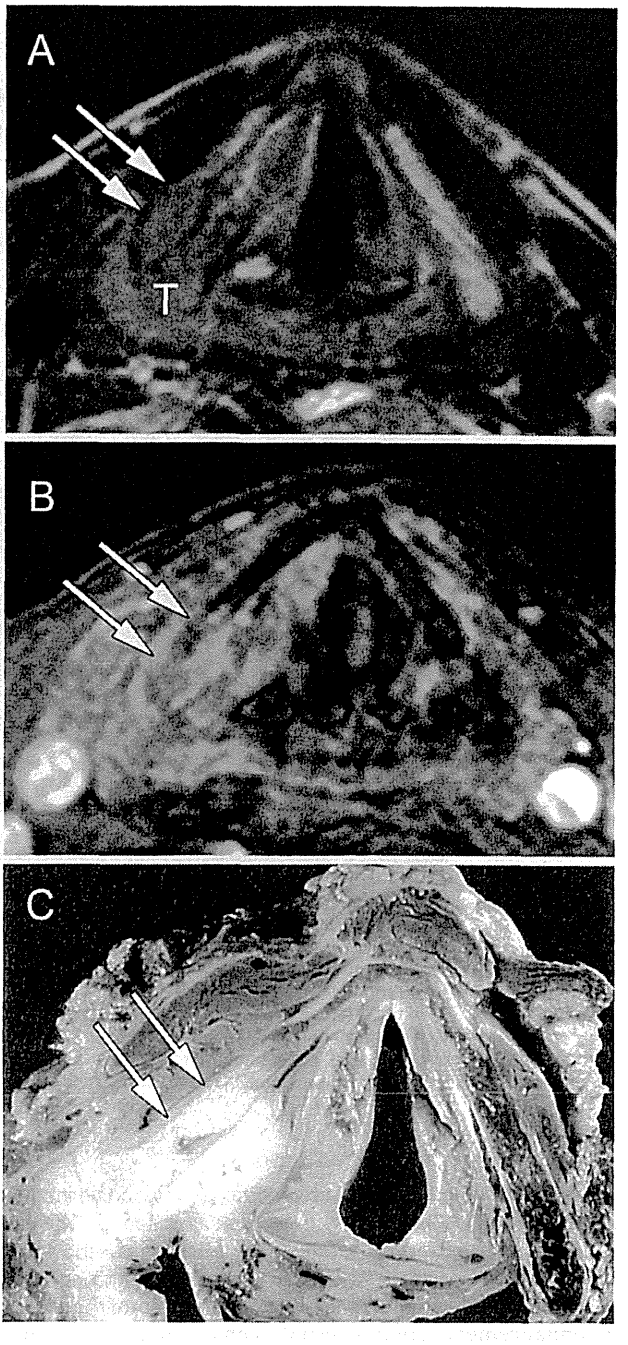

Fig. 5. Positive finding of thyroid cartilage invasion on MR imaging in a 69-year-old man with hypopharyngeal cancer. (A) Axial T2-weighted image at the level of the vocal cords shows a tumor mass (T) arising from the right piriform sinus with intermediate signal intensity. The adjacent right thyroid cartilage shows a similar signal intensity (arrows). (B) Fat-suppressed contrast-enhanced T1-weighted image shows enhancement of the tumor mass and similar enhancement of the adjacent thyroid lamina (arrows). (C) Corresponding axial slice from the surgical specimen at the same level confirms that the posterior thyroid cartilage has been invaded by the tumor cells (arrows).